Available online at www.sciencedirect.com
ScienceDirect
Journal of Sound and Vibration 320 (2009) 617–631
JOURNAL OF SOUND AND VIBRATION
www.elsevier.com/locate/jsvi

On the occurrence of flutter in the lateral–torsional instabilities of circular arches under follower loads

Noël Challamel[a,*], Charles Casandjian[a], Jean Lerbet[b]

[a] *Université Européenne de Bretagne, Laboratoire de Génie Civil et Génie Mécanique (LGCGM), INSA de Rennes, 20, avenue des Buttes de Coësmes, 35043 Rennes cedex, France*

[b] *Université d'Evry Val d'Essonne, UFR Sciences et Technologie, 40, rue du Pelvoux CE 1455, 91020 Evry Courcouronnes cedex, France*

Received 25 October 2007; received in revised form 2 August 2008; accepted 7 August 2008
Handling Editor: A.V. Metrikine
Available online 11 September 2008

Abstract

The lateral–torsional stability of circular arches subjected to radial and follower distributed loading is treated herein. Three loading cases are studied, including the radial load with constant direction, the radial load directed towards the arch centre, and the follower radial load (hydrostatic load), as treated by Nikolai in 1918. For the three cases, the buckling loads are first obtained from a static analysis. As the case of the follower radial load (hydrostatic load) is a non-conservative problem, the dynamic approach is also used to calculate the instability load. The governing equations for out-of-plane vibrations of circular arches under radial loading are then derived, both with and without Wagner's effect. Flutter instabilities may appear for sufficiently large values of opening angle, but flutter cannot occur before divergence for the parameters of interest (civil engineering applications). Therefore, it is concluded that the static approach necessarily leads to the same result as the dynamic approach, even in the non-conservative case.

1. Introduction

When an arch is loaded in its plane, the arch may buckle laterally by twisting and deflecting out of its plane, a behaviour called lateral–torsional buckling. Lateral–torsional buckling of circular arches under uniform compression (in-plane radial load—see Fig. 1) has been studied by many researchers (see, for instance, the recent papers [1,2]). In most of these studies devoted to lateral–torsional buckling, the direction of the radial load was assumed not to change, remaining in its original plane. In practice, uniform compression in a circular arch may also be produced by motion-dependent loads: the radial load may be directed towards the arch centre, or the radial load may follow its line of application. Nikolai [3] first investigated in detail the lateral–torsional buckling of circular arches under constant and follower radial loading. Nikolai [3] discussed the non-conservative behaviour of radial loading within the frame of the static criterion of stability as early as 1918 [4]. We wish to reconsider this non-conservative problem in the light of dynamics stability theory.

*Corresponding author. Tel.: +33 2 23 23 84 78; fax: +33 2 23 23 84 91.
E-mail addresses: noel.challamel@insa-rennes.fr (N. Challamel), charles.casandjian@insa-rennes.fr (C. Casandjian), jean.lerbet@ibisc.univ-evry.fr (J. Lerbet).

0022-460X/$ - see front matter © 2008 Elsevier Ltd. All rights reserved.
doi:10.1016/j.jsv.2008.08.005

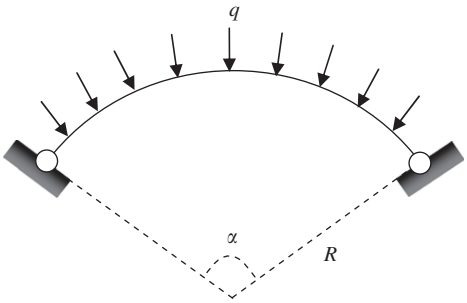

Fig. 1. Lateral–torsional buckling of circular arches under uniform compression.

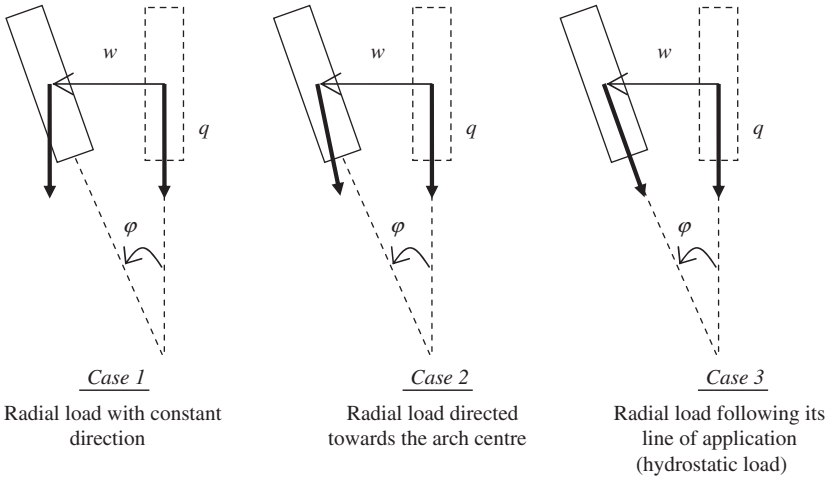

Fig. 2. Definition of the three loading cases.

Three loading cases are studied in this paper, including the radial load with constant direction (case 1), the radial load directed towards the arch centre (case 2), and the follower radial load, also called hydrostatic load (case 3) (see Figs. 1 and 2). The first theoretical results on lateral–torsional buckling of arches under uniform compression were by Nikolai [3], Federhofer [5], Hencky [6] and Timoshenko [7] for circular or narrow rectangular sections. Nikolai [3] first treated the lateral–torsional buckling of circular rings and arches under constant directional pressure (case 1) and hydrostatic load (case 3). Federhofer [5] investigated the lateral–torsional buckling of a circular ring under centrally directed pressure (case 2), by neglecting the out-of-plane bending stiffness. Hencky [6] completed Federhofer's result without this last assumption (case 2). Timoshenko [7] studied the lateral–torsional buckling of circular arches under the conservative loading of cases 1 and 2, and then extended the previous results to the arch problem. These results can be easily generalized to I-beams (see, for instance, Ref. [2]). As we will see, these two loading cases (cases 1 and 2) are conservative loading, and it is then justified to use a static stability approach to determine the buckling load. Indeed, the static and dynamic approaches lead to the same result for this conservative case. The problem is different for the follower radial load, which leads to a non-conservative problem, as explained by Farshad [8], Celep [9], and Challamel [10]. In this last case, a dynamic approach is needed to investigate the stability boundary [11]. Therefore, it is not possible to disconnect the out-of-plane stability problem and the out-of-plane vibrations problem.

The rigorous free out-of-plane vibrations of circular arches go back to the pioneering study of Michell [12] for circular sections and by neglecting the rotary inertia. Many studies have been devoted to the out-of-plane vibrations of circular arches [13–15]. An interesting feature of the governing equations is the mutual independence between the in-plane and the out-of-plane linear motions [14]. Childamparam and Leissa [16] gave a state of the art analysis of vibrations of circular arches. Research on the out-of-plane dynamics of

arches is today oriented towards the analytical treatment of the Timoshenko arc [17–19] or the treatment of arbitrarily varying cross sections [20,21].

Lateral–torsional buckling under non-conservative time-independent loading (autonomous system) has been studied by many researchers, since the pioneering work of Bolotin [22] (see, for instance, Refs. [23–34]). The dynamic approach was used in these studies of non-conservative follower loads. Lateral–torsional buckling of straight beams under distributed follower loads was formally treated by Bolotin [22]. Migliacci [23] studied the lateral–torsional instability of a simply supported beam under concentrated or distributed follower loads, and showed, in particular, that instability induced by a distributed follower load along the entire beam necessarily occurs by divergence. Ballio [25] extended these results and studied the transition from flutter to divergence instability, depending on the distributed aspect of the follower load. Moreover, Ballio [26] investigated the possibility of treating this non-conservative problem from an adjoint problem. Celep [28] exhibited flutter instabilities for cantilever beams under distributed follower loads. Lateral–torsional instability (flutter) of cantilever beams under concentrated follower forces were also investigated by Como [24], Wohlhart [27], Hodges [31], and Detinko [32]. Lateral–torsional buckling under a non-conservative follower moment was treated by Bolotin [22], Celep [29], Feodosiev [33], and Simitses and Hodges [34]. Detinko [30] also studied the case of a circular arch under an in-plane follower force. There have been very few papers devoted to lateral–torsional instabilities of arches under non-conservative follower loads (dynamics approach), except the work of Farshad [8] and Celep [9]. The study of Wasserman [35] can be also mentioned, as this study investigated the effect of the load behaviour (case 1, case 2, and case 3) on the natural frequencies of the out-of-plane vibrations. However, Wasserman [35] did not discuss the flutter occurrence for this non-conservative problem, and rotary inertia was neglected. Celep [9] obtained results in the case of combined conservative and non-conservative (follower load) distributed radial loading. Farshad [8] and Celep [9] both neglected Wagner's effect.

The lateral–torsional stability of a circular arch subjected to radial and distributed follower loading is treated herein. Three loading cases are studied, including the radial load with constant direction (case 1), the radial load directed towards the arch centre (case 2), and the follower radial load (case 3). Gravity loading (case 1) could be compared to arch bridges with very little lateral stiffness of the bridge deck, while tilt loading (case 2) occurs in bridges with a bridge deck with high lateral stiffness. Case 2 is typically encountered in stabbogen arches, where the suspended structure (e.g., bridge deck) has a greater in-plane bending stiffness than the arch rib [36]. Case 3 can be associated to a simplified model of wind load, even if it is generally admitted that such a load varies along the arc length. The elastic stability of a pair of leaning arches submitted to wind loads was studied, for instance, by Plaut and Hou [37]. Bradford and Pi [38] also mentioned some possible applications of this hydrostatic load in the case of submarine structures. Experimentally, essentially two types of loading have been tested in the literature. The gravity load (case 1 of the paper) and the radial load directed towards the arch centre (case 2 of the paper), both conservative loading, have been investigated:

- gravity load (case 1): Stüssi [39] with a rectangular cross section and
- tilt loading (case 2): Godden [36] with a circular cross section, Tokarz [40] with rectangular cross section.

Kee [41] investigated the coupled effect of a non-follower lateral load with tilt loading to take into account the wind load. La Poutré [42] recently made an extensive review of experimental testing of steel arches, and performed experimental tests on circular arches under gravity or tilt loading (case 1 and case 2 of this paper). To our knowledge, no experimental results have been published with the exact load configuration of case 3, e.g., a single uniform hydrostatic pressure. The lack of experimental results for this last case may be eventually connected to the experimental difficulties associated to the realization of some non-conservative systems (see Refs. [43,44]). Some of these difficulties may be overcome at the micro scale, as recently suggested in Ref. [45] for the implementation of follower forces in a beam-type micro-electro-mechanical systems (MEMS) resonator.

For the three cases, the buckling loads are first obtained from a static analysis, and the results of Nikolai [3] and Timoshenko [7], summarized by Farshad [8] and Wasserman [35], are then confirmed when Wagner's effect is neglected. As the case of the follower radial load (hydrostatic load—case 3) is a non-conservative problem, the dynamic approach is also used to calculate the instability load. The dynamic approach gives both

the divergence and the critical flutter loads (if the existence of these critical loads is ensured); depending on the parameters of the problem, they can be lower, higher or equal to each other. The governing equations for out-of-plane vibrations of circular arches under radial loads are derived, with the incorporation of Wagner's effect. A rigorous proof that no flutter bifurcation may occur for sufficiently small values of arch opening angle is given. Flutter instabilities may appear for larger values of the arch opening angle, but flutter cannot occur before divergence for the parameters of interest. A simple closed-form solution of the flutter load is given for the semi-circular arch. It is also shown that Wagner's effect significantly affects the flutter load in the case of flutter bifurcation. Therefore, it is concluded that the dynamic approach necessarily leads to the same result as the static approach, even in the non-conservative case. Moreover, one shows that Nikolai's solution in the case of follower loads (case 3) is still valid when Wagner's effect is taken into account.

2. Governing equations

Consider the linearized bending-torsional equations of a circular arch of radius R with a narrow rectangular cross section, acted on by a distributed radial load q. The deflection at the onset of buckling is specified by (i) the cross-section rotation angle $\varphi(x)$ in the yz plane, and (ii) the displacement $w(x)$ of the beam axis in the z direction. The effects of the pre-buckling deflections are neglected ($EI_z \gg EI_y$). Moreover, we implicitly use the independence property of the in-plane and out-of-plane vibrations (see Refs. [14,35,46]).

The variation of the strain energy ΔU, from the fundamental equilibrium state, is equal to

$$\Delta U[\varphi, w] = \frac{1}{2}\int_0^L \left(EI_y\left(w'' + \frac{\varphi}{R}\right)^2 + GJ\left(\varphi' - \frac{w'}{R}\right)^2 + \overline{N}\left(w'^2 + r_0^2\left(\varphi' - \frac{w'}{R}\right)^2\right)\right) \mathrm{d}s \quad \text{with } \overline{N} = -qR, \tag{1}$$

where GJ is the beam torsional stiffness and EI_y is the beam bending stiffness in the xz plane. The arch has an opening angle α and a length denoted by L ($L = R\alpha$).

It is worth mentioning that the term

$$\frac{1}{2}\int_0^L \overline{N} r_0^2\left(\varphi - \frac{w'}{R}\right)^2 \mathrm{d}s \tag{2}$$

is associated with the so-called Wagner's effect [47], which is responsible for the torsional buckling of doubly symmetric columns under an axial compressive load (see also Refs. [48,49]). r_0 is the cross-sectional mass radius of gyration. Wagner's effect was neglected in the previous studies dealing with the dynamics of circular arches under follower loads [8,9].

The variation of the kinetic energy is equal to

$$\Delta T[\varphi, w] = \frac{1}{2}\int_0^L \left(\mu \dot{w}^2 + \mu r_0^2 \dot{\varphi}^2\right) \mathrm{d}s, \tag{3}$$

where μ is the mass per unit length. The variation of the virtual work done by the distributed radial load is assumed to have the general form:

$$\delta \Delta W_e = -\xi_1 \int_0^L \frac{q}{R} w \delta w \, \mathrm{d}s - \xi_2 \int_0^L q \varphi \delta w \, \mathrm{d}s. \tag{4}$$

The three cases presented in the introduction are covered by such an expression (see also Ref. [8]). Case 1 is obtained with $\xi_1 = 0$ and $\xi_2 = 0$ (radial load with constant direction). Case 2 is obtained with $\xi_1 = 1$ and $\xi_2 = 0$ (radial load directed towards the arch centre). Finally, Case 3 is obtained with $\xi_1 = 0$ and $\xi_2 = 1$ (follower radial load or hydrostatic load). The first term of Eq. (4) derives from a potential, whereas the second term of Eq. (4) cannot derive from a potential, as detailed in Ref. [10]. As a consequence, the conservativeness criterion is simply reduced to

$$\xi_2 = 0 \Leftrightarrow \text{conservative problem}. \tag{5}$$

The dynamic equations are obtained via the Hamilton principle:

$$\int_{t_1}^{t_2} (\delta\Delta U - \delta\Delta T - \delta\Delta W_e)\,\mathrm{d}t = 0. \tag{6}$$

The partial differential equations are finally

$$\begin{vmatrix} \mu\ddot{w} + EI_y\left(w^{(4)} + \frac{\varphi''}{R}\right) + \frac{GJ - qRr_0^2}{R}\left(\varphi'' - \frac{w''}{R}\right) + qRw'' + \xi_1\frac{q}{R}w + \xi_2 q\varphi = 0, \\ \mu r_0^2\ddot{\varphi} + \frac{EI_y}{R}\left(w'' + \frac{\varphi}{R}\right) - (GJ - qRr_0^2)\left(\varphi'' - \frac{w''}{R}\right) = 0. \end{vmatrix} \tag{7}$$

A solution is sought in the form:

$$w = R\overline{w}\mathrm{e}^{\Omega t} \quad \text{and} \quad \varphi = \phi\mathrm{e}^{\Omega t}. \tag{8}$$

The four dimensionless parameters may be introduced as

$$p = \frac{qR^3}{EI_y}, \quad \lambda = \frac{EI_y}{GJ}, \quad \overline{r} = \frac{r_0}{R} \quad \text{and} \quad \Lambda^2 = \frac{R^4\mu\Omega^2}{EI_y}. \tag{9}$$

Moreover, the spatial derivative with respect to s is expressed in terms of the polar coordinate θ, leading to the new dimensionless differential equations:

$$\begin{vmatrix} \lambda\overline{w}^{(4)} + (p\lambda - 1 + p\lambda\overline{r}^2)\overline{w}'' + \overline{w}(\lambda\Lambda^2 + \xi_1 p\lambda) + (\lambda + 1 - p\lambda\overline{r}^2)\phi'' + \lambda\xi_2 p\phi = 0, \\ (\lambda + 1 - p\lambda\overline{r}^2)\overline{w}'' - (1 - p\lambda\overline{r}^2)\phi'' + \phi(\lambda + \lambda\Lambda^2\overline{r}^2) = 0. \end{vmatrix} \tag{10}$$

The second equation of Eq. (10) leads to

$$\overline{w}'' = \frac{1 - p\lambda\overline{r}^2}{1 + \lambda - p\lambda\overline{r}^2}\phi'' - \frac{\lambda}{1 + \lambda - p\lambda\overline{r}^2}(1 + \Lambda^2\overline{r}^2)\phi. \tag{11}$$

Inserting Eq. (11) into the first equation of Eq. (10) leads to the sixth-order linear differential equation of one variable ϕ:

$$\begin{aligned} &(1 - p\lambda\overline{r}^2)\phi^{(6)} + [(p + 2)(1 - p\lambda\overline{r}^2) - \lambda\Lambda^2\overline{r}^2]\phi^{(4)} + [(1 + \Lambda^2\overline{r}^2)(1 - p\lambda\overline{r}^2 - \lambda p) \\ &\quad + (\Lambda^2 + \xi_1 p)(1 - p\lambda\overline{r}^2) + \xi_2 p(1 - p\lambda\overline{r}^2 + \lambda)]\phi'' - \lambda(1 + \Lambda^2\overline{r}^2)(\Lambda^2 + \xi_1 p)\phi = 0. \end{aligned} \tag{12}$$

Some particular cases can be deduced from Eq. (12). First, it can be useful to derive this differential equation when Wagner's effect is neglected (as already considered in Refs. [8,9,35]):

$$\phi^{(6)} + (p + 2 - \lambda\Lambda^2\overline{r}^2)\phi^{(4)} + [(1 + \Lambda^2\overline{r}^2)(1 - \lambda p) + \Lambda^2 + \xi_1 p + \xi_2 p(1 + \lambda)]\phi'' - \lambda(1 + \Lambda^2\overline{r}^2)(\Lambda^2 + \xi_1 p)\phi = 0. \tag{13}$$

Free vibrations are obtained by setting $p = 0$ and $\omega^2 = -\Lambda^2$:

$$\phi^{(6)} + (2 + \lambda\omega^2\overline{r}^2)\phi^{(4)} + [1 - \omega^2(1 + \overline{r}^2)]\phi'' + \lambda\omega^2(1 - \omega^2\overline{r}^2)\phi = 0. \tag{14}$$

This sixth-order differential equation was given, for instance, by Lee and Chao [21]. The particular case with $\overline{r} = 0$ leads to the much simpler case (see Ref. [14]):

$$\phi^{(6)} + 2\phi^{(4)} + (1 - \omega^2)\phi'' + \lambda\omega^2\phi = 0. \tag{15}$$

Solution of the general linear differential equation (Eq. (12)) is written as

$$\phi(\theta) = \sum_{i=1}^{6} C_i\mathrm{e}^{\beta_i\theta}, \tag{16}$$

where β_i are assumed to be the simple roots of the characteristic equation, obtained from the introduction of Eq. (16) into Eq. (12):

$$(1-p\lambda\bar{r}^2)\beta^6+[(p+2)(1-p\lambda\bar{r}^2)-\lambda\Lambda^2\bar{r}^2]\beta^4+[(1+\Lambda^2\bar{r}^2)(1-p\lambda\bar{r}^2-\lambda p)+(\Lambda^2+\xi_1 p)(1-p\lambda\bar{r}^2)+\xi_2 p(1-p\lambda\bar{r}^2+\lambda)]\beta^2-\lambda(1+\Lambda^2\bar{r}^2)(\Lambda^2+\xi_1 p)=0. \tag{17}$$

It can be useful to introduce the change of variable $\gamma=\beta^2$, in order to convert the characteristic equation into a third-order polynomial expression:

$$(1-p\lambda\bar{r}^2)\gamma^3+[(p+2)(1-p\lambda\bar{r}^2)-\lambda\Lambda^2\bar{r}^2]\gamma^2+[(1+\Lambda^2\bar{r}^2)(1-p\lambda\bar{r}^2-\lambda p)+(\Lambda^2+\xi_1 p)(1-p\lambda\bar{r}^2)+\xi_2 p(1-p\lambda\bar{r}^2+\lambda)]\gamma-\lambda(1+\Lambda^2\bar{r}^2)(\Lambda^2+\xi_1 p)=0. \tag{18}$$

As described by Hencky [6] and Howson and Jemah [18], the solution of such equations can be achieved by reduction of Cardan's form.

3. Static approach—conservative problem—Wagner's effect neglected

The static approach leads to the exact buckling load (in the stability sense of Lyapunov) for conservative systems. Indeed, this approach can be rigorously applied to the case $\xi_2=0$. For the static approach, the parameter Λ is assumed to vanish. When Wagner's effect is neglected, the characteristic equation (Eq. (18)) is then converted into

$$\gamma^3+(p+2)\gamma^2+(1-\lambda p+\xi_1 p)\gamma-\lambda\xi_1 p=0. \tag{19}$$

Simple closed-form solutions can be obtained for case 1 and case 2. Case 2 is first treated ($\xi_1=1$). The characteristic equation (Eq. (19)) can be rewritten in the following form:

$$(\gamma+1)(\gamma^2+(p+1)\gamma-p\lambda)=0. \tag{20}$$

The third real solutions of this factorized equation are finally obtained:

$$(\gamma_1,\gamma_2,\gamma_3)=\left(-\frac{\sqrt{(p+1)^2+4p\lambda}+p+1}{2},\frac{\sqrt{(p+1)^2+4p\lambda}-(p+1)}{2},-1\right). \tag{21}$$

The solution of Eq. (13) is then written as

$$\phi(\theta)=C_1\cos(\sqrt{-\gamma_1}\theta)+C_2\sin(\sqrt{-\gamma_1}\theta)+C_3\cosh(\sqrt{\gamma_2}\theta)+C_4\sinh(\sqrt{\gamma_2}\theta)+C_5\cos\theta+C_6\sin\theta, \tag{22}$$

where (C_i) are real constants. To proceed further, one may consider the boundary conditions of the pin-ended arch, the ends of which are restrained against lateral displacement ($\overline{w}=0$), against rotation ($\phi=0$), and with bending moment M_y vanishing (and then $\overline{w}''=0$). The 6 boundary conditions associated with the eigenmode of the laterally pin-ended arch are:

$$\phi(\theta)=0 \text{ for } \theta=0,\alpha;\quad \phi''(\theta)=0 \text{ for } \theta=0,\alpha;\quad \phi^{(4)}(\theta)=0 \text{ for } \theta=0,\alpha. \tag{23}$$

Introducing the boundary conditions (Eq. (23)) into the eigenmode formulation (Eq. (22)) leads to the eigenvalue equation:

$$\sin\left(\sqrt{-\gamma_1}\alpha\right)\sinh\left(\sqrt{\gamma_2}\alpha\right)\sin\alpha=0\Rightarrow\left|\begin{array}{l}\alpha=n\pi,\\ \sqrt{-\gamma_1}\alpha=n\pi.\end{array}\right. \tag{24}$$

The first mode is the rigid mode associated with the semi-circular arch, whereas the second family of buckling loads is written as

$$p_n=(n\pi)^2\frac{(n\pi)^2-\alpha^2}{\alpha^2((n\pi)^2+\lambda\alpha^2)}. \tag{25}$$

Case 1 is now analysed ($\xi_1 = 0$). In this case, the sixth-order differential equation (Eq. (13)) can be reduced to a fourth-order differential equation from the boundary conditions (Eq. (23)):

$$\phi^{(4)} + (p+2)\phi'' + (1-\lambda p)\phi = 0. \tag{26}$$

One recognizes the fourth-order differential equation given by Timoshenko [7]. The characteristic equation is then written as

$$\gamma^2 + (p+2)\gamma + (1-\lambda p) = 0 \tag{27}$$

with the two real solutions detailed as

$$(\gamma_1, \gamma_2) = \left(-\frac{\sqrt{(p+2)^2 + 4p\lambda - 4} + p + 2}{2}, \frac{\sqrt{(p+2)^2 + 4p\lambda - 4} - (p+2)}{2} \right). \tag{28}$$

Two types of solutions must be distinguished, depending on the sign of γ_2. First, it is assumed that $p \geqslant 1/\lambda$ ($\gamma_2 \geqslant 0$). The solution of Eq. (26) is then written as

$$\phi(\theta) = C_1 \cos\left(\sqrt{-\gamma_1}\theta\right) + C_2 \sin\left(\sqrt{-\gamma_1}\theta\right) + C_3 \cosh\left(\sqrt{\gamma_2}\theta\right) + C_4 \sinh\left(\sqrt{\gamma_2}\theta\right). \tag{29}$$

Introducing the boundary conditions (Eq. (23)) into the eigenmode formulation (Eq. (29)) leads to the eigenvalue equation:

$$\sin\left(\sqrt{-\gamma_1}\alpha\right) \sinh\left(\sqrt{\gamma_2}\alpha\right) = 0 \Rightarrow \sqrt{-\gamma_1}\alpha = n\pi. \tag{30}$$

The second case of Timoshenko's problem is based on $p \leqslant 1/\lambda$ ($\gamma_2 \leqslant 0$). It is worth mentioning that this case was not treated by Timoshenko [7]. The solution of Eq. (26) is then written as

$$\phi(\theta) = C_1 \cos\left(\sqrt{-\gamma_1}\theta\right) + C_2 \sin\left(\sqrt{-\gamma_1}\theta\right) + C_3 \cos\left(\sqrt{-\gamma_2}\theta\right) + C_4 \sin\left(\sqrt{-\gamma_2}\theta\right). \tag{31}$$

Introducing the boundary conditions (Eq. (23)) into the eigenmode formulation (Eq. (31)) leads to the eigenvalue equation:

$$\sin\left(\sqrt{-\gamma_1}\alpha\right) \sin\left(\sqrt{-\gamma_2}\alpha\right) = 0 \Rightarrow \left| \begin{array}{l} \sqrt{-\gamma_1}\alpha = n\pi, \\ \sqrt{-\gamma_2}\alpha = n\pi, \end{array} \right. \quad \text{with } \sqrt{-\gamma_1} \geqslant \sqrt{-\gamma_2}. \tag{32}$$

Eq. (32) leads to the same family of buckling loads (see Eq. (30)):

$$p_n = \frac{((n\pi)^2 - \alpha^2)^2}{\alpha^2((n\pi)^2 + \lambda\alpha^2)}. \tag{33}$$

4. Non-conservative problem—static approach—Wagner's effect neglected

As for case 2 (Timoshenko's problem), the sixth-order differential equation of case 3 (hydrostatic load) ($\xi_1 = 0$, $\xi_2 = 1$) can be reduced to a fourth-order differential equation:

$$\phi^{(4)} + (p+2)\phi'' + (1+p)\phi = 0. \tag{34}$$

The characteristic equation is then written as

$$\gamma^2 + (p+2)\gamma + (1+p) = 0. \tag{35}$$

with the two real solutions detailed as

$$(\gamma_1, \gamma_2) = (-1-p, -1). \tag{36}$$

The solution of Eq. (34) is then obtained as

$$\phi(\theta) = C_1 \cos(\sqrt{p+1}\,\theta) + C_2 \sin(\sqrt{p+1}\,\theta) + C_3 \cos(\theta) + C_4 \sin(\theta). \tag{37}$$

Introducing the boundary conditions (Eq. (23)) into the eigenmode formulation (Eq. (37)) leads to the eigenvalue equation:

$$\sin(\sqrt{p+1}\alpha)\sin(\alpha)=0 \Rightarrow \left| \begin{array}{l} \alpha = n\pi, \\ \sqrt{p+1}\alpha = n\pi. \end{array} \right. \tag{38}$$

The first mode is the rigid mode associated with the semi-circular arch, whereas the second family of "static" buckling loads is written as

$$p_n = \left(\frac{n\pi}{\alpha}\right)^2 - 1. \tag{39}$$

It is remarkable that this value is exactly the buckling value of the fundamental in-plane buckling for $n=2$ (see, for instance, Refs. [34,46]). Therefore, it appears that the follower load problem leads to the coincidence of the fundamental in-plane buckling problem and the second buckling value of the out-of-plane buckling problem ($n=2$).

The dimensionless fundamental buckling load $\overline{p}=p_1(\alpha/\pi)^2$ can be introduced. The three cases can be summarized as follows (see also Nikolai [3], Timoshenko [7], and more recently Farshad [8] and Wasserman [35]):

$$\left| \begin{array}{l} (\xi_1,\xi_2)=(0,0) \Rightarrow \overline{p}=\dfrac{(\pi^2-\alpha^2)^2}{\pi^2(\pi^2+\lambda\alpha^2)}, \\ (\xi_1,\xi_2)=(1,0) \Rightarrow \overline{p}=\dfrac{\pi^2-\alpha^2}{\pi^2+\lambda\alpha^2}, \\ (\xi_1,\xi_2)=(0,1) \Rightarrow \overline{p}=1-\dfrac{\alpha^2}{\pi^2} \end{array} \right. \tag{40}$$

with $\lambda=(1+\upsilon)/2$ for thin rectangular beam and υ is the Poisson's ratio.

The buckling solutions for $\xi_2=0$ (case 1 and case 2 are conservative cases) are the rigorous bifurcation solutions (the static approach is equivalent to the dynamic approach), whereas the last solution, corresponding to the non-conservative Nikolai's problem (case 3), is only obtained from a static point of view (divergence load). The proof of the loss of stability must be completed by a dynamic approach in order to study the occurrence of flutter. The evolution of $\overline{p}$ versus α is shown in Fig. 3. It is remarkable that Nikolai's solution

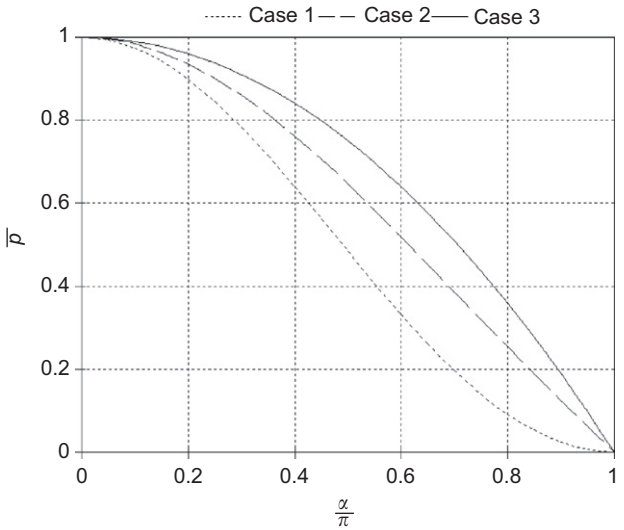

Fig. 3. Comparison of the dimensionless buckling load $\overline{p}$ versus the opening angle α; $\lambda=0.65$ (thin rectangular section with $\upsilon=0.3$); $\alpha\in[0;\pi]$.

does not depend on λ (and, as a consequence, on Poisson's ratio υ). As remarked by Wasserman [35], and more recently by Pi et al. [2], the buckling load of case 3 is the highest, while the buckling load of case 1 is the lowest. Moreover, buckling is controlled by the second mode ($n=2$) of the arch for α greater than $3\pi/2$ in case 1 (as described by Celep [9]). For case 2 and case 3, a jump appears at α equal to π (abrupt transition from the fundamental buckling mode to the second mode).

5. Dynamic approach—non-conservative problem—Wagner's effect neglected

It is assumed that the solution of Eq. (13) is written as

$$\phi = \phi_0 \sin\left(n\pi\frac{\theta}{\alpha}\right). \tag{41}$$

It is easily checked that this solution verifies the boundary conditions (Eq. (23)). Inserting Eq. (41) into Eq. (13) leads to

$$\begin{aligned}&\lambda\bar{r}^2\Lambda^4 + \left[\lambda\bar{r}^2\left(\frac{n\pi}{\alpha}\right)^4 + \bar{r}^2(1-\lambda p)\left(\frac{n\pi}{\alpha}\right)^2 + \left(\frac{n\pi}{\alpha}\right)^2 + \lambda + \lambda\bar{r}^2\xi_1 p\right]\Lambda^2\\ &+ \left[\left(\frac{n\pi}{\alpha}\right)^6 - (2+p)\left(\frac{n\pi}{\alpha}\right)^4 + (1-\lambda p)\left(\frac{n\pi}{\alpha}\right)^2 + (\xi_1 p + \xi_2 p(1+\lambda))\left(\frac{n\pi}{\alpha}\right)^2 + \lambda\xi_1 p\right] = 0.\end{aligned} \tag{42}$$

The free vibration modes ($\omega^2 = -\Lambda^2$) are obtained from Eq. (42), and were given by Michell [12] for a semi-circular arch when the rotary is neglected (see also Ref. [50]):

$$\bar{r} = 0 \text{ and } p = 0 \Rightarrow \omega_n^2 = \left(\frac{n\pi}{\alpha}\right)^2 \frac{((n\pi/\alpha)^2-1)^2}{(n\pi/\alpha)^2+\lambda}. \tag{43}$$

For the non-conservative case (ξ_1, ξ_2) = (0, 1), Eq. (42) can formally be written as

$$a\Lambda^4 + b\Lambda^2 + c = 0 \quad \text{with} \quad \left|\begin{array}{l} a = \lambda\bar{r}^2,\\ b = \lambda\bar{r}^2\left(\frac{n\pi}{\alpha}\right)^4 + \bar{r}^2(1-\lambda p)\left(\frac{n\pi}{\alpha}\right)^2 + \left(\frac{n\pi}{\alpha}\right)^2 + \lambda,\\ c = \left(\frac{n\pi}{\alpha}\right)^6 - (2+p)\left(\frac{n\pi}{\alpha}\right)^4 + (1+p)\left(\frac{n\pi}{\alpha}\right)^2. \end{array}\right. \tag{44}$$

The flutter bifurcation is reached for

$$\Delta = b^2 - 4ac = 0. \tag{45}$$

Application of criterion (Eq. (45)) leads to the polynomial expression:

$$\begin{aligned}&p^2\left[\lambda^2\bar{r}^4\left(\frac{n\pi}{\alpha}\right)^4\right] + p\left[-2\lambda\bar{r}^2\left(\frac{n\pi}{\alpha}\right)^2\left(\lambda\bar{r}^2\left(\frac{n\pi}{\alpha}\right)^4 + \bar{r}^2\left(\frac{n\pi}{\alpha}\right)^2 - \left(\frac{n\pi}{\alpha}\right)^2 + \lambda + 2\right)\right]\\ &+ \left[\left(\lambda\bar{r}^2\left(\frac{n\pi}{\alpha}\right)^4 + \bar{r}^2\left(\frac{n\pi}{\alpha}\right)^2 + \left(\frac{n\pi}{\alpha}\right)^2 + \lambda\right)^2 - 4\lambda\bar{r}^2\left(\frac{n\pi}{\alpha}\right)^2\left(\left(\frac{n\pi}{\alpha}\right)^2 - 1\right)^2\right] = 0.\end{aligned} \tag{46}$$

The fundamental question related to the appearance of the flutter phenomenon concerns the existence of a real positive root to this second-order polynomial equation. Eq. (46) is a second-order polynomial expression of p, whose discriminant δ can be calculated from

$$\begin{aligned}\delta = {}& 4\lambda^2\bar{r}^4\left(\frac{n\pi}{\alpha}\right)^4\left[\lambda\bar{r}^2\left(\frac{n\pi}{\alpha}\right)^4 + \bar{r}^2\left(\frac{n\pi}{\alpha}\right)^2 - \left(\frac{n\pi}{\alpha}\right)^2 + \lambda + 2\right]^2 - 4\lambda^2\bar{r}^4\left(\frac{n\pi}{\alpha}\right)^4\\ &\times\left[\left(\lambda\bar{r}^2\left(\frac{n\pi}{\alpha}\right)^4 + \bar{r}^2\left(\frac{n\pi}{\alpha}\right)^2 + \left(\frac{n\pi}{\alpha}\right)^2 + \lambda\right)^2 - 4\lambda\bar{r}^2\left(\frac{n\pi}{\alpha}\right)^2\left(\left(\frac{n\pi}{\alpha}\right)^2 - 1\right)^2\right].\end{aligned} \tag{47}$$

The discriminant δ can be simplified as

$$\delta = 16\lambda^2\bar{r}^4\left(\frac{n\pi}{\alpha}\right)^4\left(1-\left(\frac{n\pi}{\alpha}\right)^2\right)(1+\lambda)\left(1+\bar{r}^2\left(\frac{n\pi}{\alpha}\right)^2\right). \tag{48}$$

As a consequence,

$$\alpha<\pi \Rightarrow \delta<0. \tag{49}$$

This means that Eq. (46) has no real solution of the dimensionless load parameter p for $\alpha<\pi$, and thus the flutter phenomenon cannot occur for $\alpha<\pi$. It appears that the flutter phenomenon cannot occur for this system, and the bifurcation criterion $c=0$ leads to a divergence type of instability. Eq. (39) is found again, and the dynamic and the static criteria lead to the same boundary of the stability load. Although this problem is intrinsically a non-conservative problem, it can be classified by Leipholz as a conservative system of the second kind. This problem is analogous to the one of Pflüger's rod, a non-conservative problem under a distributed follower load, whose stability boundary is also ruled by a static approach [51–53]. A special case is obtained for a semi-circular arch with n equal to 1:

$$\alpha=\pi \Rightarrow \delta=0 \quad \text{for } n=1. \tag{50}$$

In this case, the flutter load obtained from Eq. (46) is equal to

$$\alpha=\pi \Rightarrow p_1=\frac{(\lambda+1)(\bar{r}^2+1)}{\lambda\bar{r}^2}. \tag{51}$$

This flutter load depends also on the rotary inertia, and approaches an infinite value when the rotary inertia tends towards zero. In fact, flutter cannot occur when the rotary inertia is neglected ($\bar{r}=0$), as considered, for instance, by Wasserman [35]. The possibility of flutter for a semi-circular arch under follower loads was first recognized by Farshad [8], although the value of the bifurcation load presented herein is different from the one of Farshad [8] (except for $\bar{r}^2=2$). Our values agree with those of Celep [9] when Wagner's effect is neglected, even if Celep did not propose a closed-form solution for $\alpha=\pi$. This flutter bifurcation is more clearly highlighted for large values of opening angle $\alpha\in[\pi;2\pi]$:

$$\alpha\in[\pi;2\pi] \Rightarrow p_{1,2}=\frac{\lambda\bar{r}^2(\pi/\alpha)^4+\bar{r}^2(\pi/\alpha)^2-(\pi/\alpha)^2+\lambda+2\pm2\sqrt{1-(\pi/\alpha)^2}\sqrt{1+\lambda}\sqrt{1+\bar{r}^2(\pi/\alpha)^2}}{\lambda\bar{r}^2(\pi/\alpha)^2}. \tag{52}$$

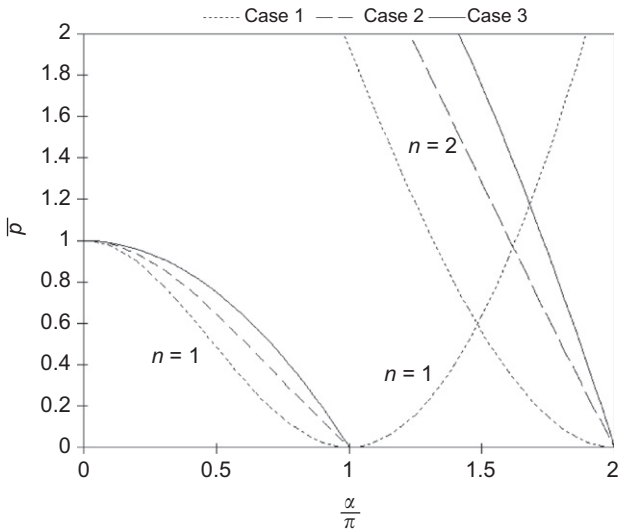

Fig. 4. Comparison of the dimensionless buckling load $\overline{p}$ versus the opening angle α; $\lambda=0.65$ (thin rectangular section with $\upsilon=0.3$); $\alpha\in[0;2\pi]$.

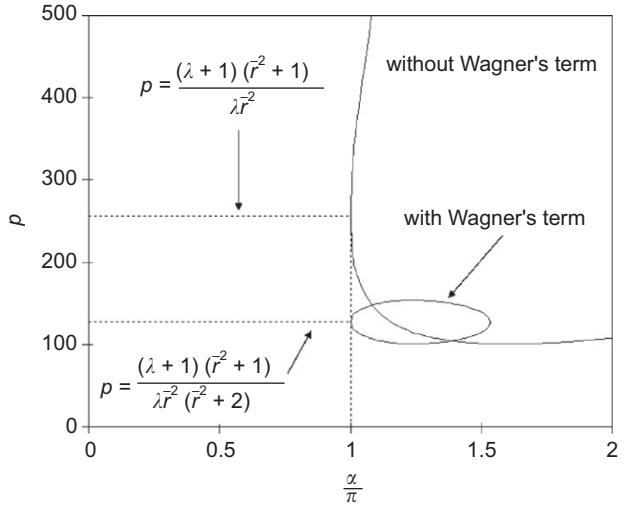

Fig. 5. Flutter load versus the opening angle α; $\lambda = 0.65$ (thin rectangular section with $\upsilon = 0.3$) and $\bar{r} = 0.1$; $\alpha \in [0;2\pi]$; case 3 (hydrostatic load)–nonconservative case.

However, it can be shown that these flutter loads (and in particular the smallest one) are much larger than the buckling loads obtained from the static approach, even for $\alpha \in [\pi;\ 2\pi]$ (see Fig. 4). Fig. 5 shows the evolution of the flutter load versus the opening angle, and the typical turning point for the semi-circular arch problem ($\alpha = \pi$).

6. Incorporation of Wagner's effect

The previous results may easily be extended to the case when Wagner's effect is taken into account (see Eq. (12)). For the two conservative cases (case 1 and case 2), the static approach leads to a second-order polynomial expression, detailed below for case 1 $(\xi_1,\ \xi_2) = (0,\ 0)$:

$$\lambda\bar{r}^2 p^2 + \left[-\lambda\bar{r}^2\left(\frac{n\pi}{\alpha}\right)^2\left(1-\left(\frac{\alpha}{n\pi}\right)^2\right)^2 - \left(1+\lambda\left(\frac{\alpha}{n\pi}\right)^2\right)\right]p + \left(\frac{n\pi}{\alpha}\right)^2\left(1-\left(\frac{\alpha}{n\pi}\right)^2\right)^2 = 0. \tag{53}$$

For case 2 $(\xi_1,\ \xi_2) = (1,\ 0)$, the second-order polynomial expression is given by

$$\lambda\bar{r}^2 p^2 + \left[\lambda\bar{r}^2\left(1-\left(\frac{n\pi}{\alpha}\right)^2\right) - \left(1+\lambda\left(\frac{\alpha}{n\pi}\right)^2\right)\right]p + \left(\frac{n\pi}{\alpha}\right)^2 - 1 = 0. \tag{54}$$

Finally, for case 3 $(\xi_1,\ \xi_2) = (0,\ 1)$, the second-order polynomial expression can be factorized by

$$(\lambda p\bar{r}^2 - 1)\left(p - \left[\left(\frac{n\pi}{\alpha}\right)^2 - 1\right]\right) = 0. \tag{55}$$

These three expressions were obtained by Pi et al. [2]. Eq. (40) is a particular case of Eqs. (53)–(55) when $\bar{r}$ is sufficiently small. It is worth mentioning that the incorporation of Wagner's term is imperceptible for thin rectangular beams, and the result summarized in Eq. (40) is more readable for engineering applications. Moreover, the static approach associated with case 3 $(\xi_1,\ \xi_2) = (0,\ 1)$, the non-conservative case, exactly leads to Eq. (39). A second uncoupled torsional mode is obtained for p equal to $1/(\lambda\bar{r}^2)$, that is $\overline{N}$ equal to $-GJ/r_0^2$, but the associated buckling value associated with this mode is generally much larger than the other one. Therefore, Wagner's effect does not affect this instability load (instability by divergence). In this case, the buckling load is that derived by Nikolai [3], and is independent of both λ and $\bar{r}$ (even if Wagner's term is explicitly introduced in the governing equations).

The dynamics approach must also be corrected to evaluate the flutter boundary in this last case. Inserting the postulated form of ϕ (Eq. (41)) into the differential equation (Eq. (12)) leads to the frequency equation:

$$a\Lambda^4 + b\Lambda^2 + c = 0 \quad \text{with} \quad \begin{cases} a = \lambda\bar{r}^2, \\ b = \lambda\bar{r}^2\left(\frac{n\pi}{\alpha}\right)^4 + \bar{r}^2(1-\lambda p\bar{r}^2-\lambda p)\left(\frac{n\pi}{\alpha}\right)^2 + \left(\frac{n\pi}{\alpha}\right)^2(1-\lambda p\bar{r}^2) + \lambda, \\ c = (1-\lambda p\bar{r}^2)\left(\frac{n\pi}{\alpha}\right)^6 - (2+p)\left(\frac{n\pi}{\alpha}\right)^4(1-\lambda p\bar{r}^2) + (1+p)\left(\frac{n\pi}{\alpha}\right)^2(1-\lambda p\bar{r}^2). \end{cases} \tag{56}$$

The flutter criterion (Eq. (45)) leads to the polynomial expression:

$$p^2\lambda^2\bar{r}^4\left(\frac{n\pi}{\alpha}\right)^2\left[\left(\frac{n\pi}{\alpha}\right)^2\bar{r}^2(4+\bar{r}^2)+4\right] + p\left[-2\lambda\bar{r}^2\left(\frac{n\pi}{\alpha}\right)^2\left(\lambda\bar{r}^4\left(\frac{n\pi}{\alpha}\right)^4 + \left(\frac{n\pi}{\alpha}\right)^2(\bar{r}^2(3+4\lambda)+\bar{r}^4) + (2\lambda+2-\lambda\bar{r}^2)\right)\right]$$
$$+\left[\left(\lambda\bar{r}^2\left(\frac{n\pi}{\alpha}\right)^4 + \bar{r}^2\left(\frac{n\pi}{\alpha}\right)^2 + \left(\frac{n\pi}{\alpha}\right)^2 + \lambda\right)^2 - 4\lambda\bar{r}^2\left(\frac{n\pi}{\alpha}\right)^2\left(\left(\frac{n\pi}{\alpha}\right)^2 - 1\right)^2\right] = 0. \tag{57}$$

Moreover, the discriminant δ can be simplified as

$$\delta = 16\lambda^2\bar{r}^4\left(\frac{n\pi}{\alpha}\right)^2\left(1-\left(\frac{n\pi}{\alpha}\right)^2\right)\left[\lambda^2\bar{r}^6\left(\frac{n\pi}{\alpha}\right)^8 + \lambda\bar{r}^4(-\lambda\bar{r}^2-2+\lambda)\left(\frac{n\pi}{\alpha}\right)^6 + \bar{r}^2(1-2\lambda)(1+\lambda\bar{r}^2)\left(\frac{n\pi}{\alpha}\right)^4\right.$$
$$\left.+(1+\bar{r}^2\lambda(1-2\lambda))\left(\frac{n\pi}{\alpha}\right)^2 - \lambda^2\right]. \tag{58}$$

Eq. (58) shows that flutter phenomenon cannot occur for $\alpha<\pi$. As previously seen in the absence of Wagner's effect, the discriminant δ vanishes for the first mode associated with the semi-circular arch ($n=1$, $\alpha=\pi$). The comparison of the flutter load with and without Wagner's effect is shown in Figs. 5 and 6. The typical turning point for the semi-circular arch problem ($\alpha=\pi$) is also observed. This characteristic flutter load, incorporating Wagner's effect, is equal to

$$\alpha = \pi \Rightarrow p_1 = \frac{(\lambda+1)(\bar{r}^2+1)}{\lambda\bar{r}^2(\bar{r}^2+2)}. \tag{59}$$

The ratio between this value and that obtained without Wagner's term is equal to $1/(2+\bar{r}^2)$, and is close to half for sufficiently small values of $\bar{r}$. Clearly, Wagner's phenomenon has a meaningful destabilizing effect from the dynamics point of view. Moreover, the shape of the flutter boundary is affected by Wagner's term, as it actually is characterized by a closed loop (Fig. 5).

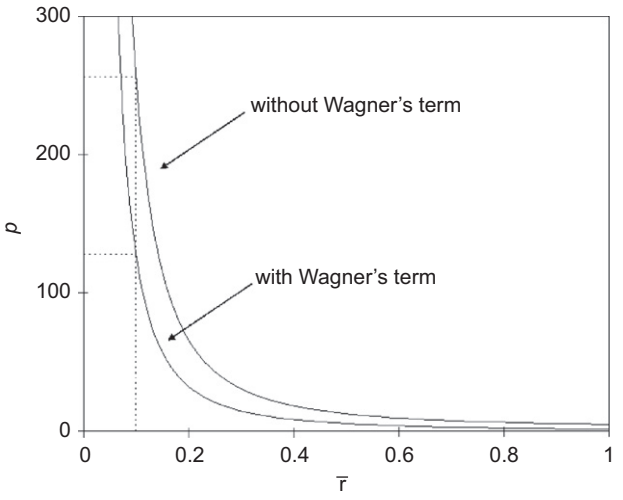

Fig. 6. Flutter load versus $\bar{r}$; $\lambda = 0.65$ (thin rectangular section with $\upsilon = 0.3$); $\alpha = \pi$; case 3 (hydrostatic load)–nonconservative case.

Finally, it can be concluded that flutter cannot occur for the present case of lateral–torsional buckling of arches under non-conservative follower loads, except in some very specific cases (for the semi-circular arch, for instance). Even for these cases, flutter cannot occur before divergence for the parameters of interest (those in practical civil engineering applications). This means that a static approach can be used for this problem, even if the problem is non-conservative. Nevertheless, flutter occurrence could be predominant for large values of $\overline{r}$, and for large values of opening angle α, which could be encountered in micromechanical applications (see Fig. 6).

7. Conclusions

The lateral–torsional stability of circular arches subjected to radial and follower distributed loads is treated herein. Three load cases are studied, including the radial load with constant direction (case 1), the radial load directed towards the arch centre (case 2), and the follower radial load (case 3). For the three cases, the buckling loads are first obtained from a static analysis, and the results of Nikolai [3] and Timoshenko [7], summarized by Farshad [8] and Wasserman [35], are then confirmed when Wagner's effect is neglected. These results are extended to the case when Wagner's effect is taken into account, and the results of Pi et al. [2] are confirmed.

As the case of the follower radial load (Nikolai's problem) is a fully intrinsically non-conservative problem, the dynamic approach is also used to calculate the instability load. The governing equations for out-of-plane vibrations of circular arches under radial loads are then derived with the incorporation of Wagner's effect. A rigorous proof that no flutter bifurcation may occur for sufficiently small values of arch opening angle is given ($\alpha < \pi$). In this case, although this problem is intrinsically a non-conservative problem, it can be classified by Leipholz as a conservative system of the second kind [4,51]. Flutter instabilities may appear for larger values of the arch opening angle, but flutter cannot occur before divergence for the parameters of interest (those for practical civil engineering applications). A simple closed-form solution of the flutter load is given for the semi-circular arch. It is also shown that Wagner's effect significantly affects the flutter load in the case of flutter bifurcation.

Therefore, it is concluded that the dynamic approach necessarily leads to the same result as the static approach, even in the non-conservative case. Furthermore, Wagner's term generally has no influence on the buckling load (divergence load) in case 3 (non-conservative follower loading). Nikolai's buckling load, obtained 90 years ago, still remains valuable for this undamped non-conservative problem, even if the introduction of damping could strongly affect these results (see, for instance, Ref. [22] and more recently, Refs.[54,55]).

References

[1] N.H. Lim, Y.J. Kang, Out of plane stability of circular arches, *International Journal of Mechanical Sciences* 46 (2004) 1115–1137.
[2] Y.L. Pi, M.A. Bradford, N.S. Trahair, Y.Y. Chen, A further study of flexural-torsional buckling of elastic arches, *International Journal of Structural Stability and Dynamics* 5 (2) (2005) 163–183.
[3] E.L. Nikolai, On the stability of a circular ring and of a circular arch under uniformly distributed normal loading (in Russian), *Izv. Petrogradskogo Polit. Inst.* 27 (1918) (cited by Gajewski and Zyczkowski, 1988 [4]) – see also *Trudi po mehanike*, 278–328, 1955 (cited by Wasserman, 1978 [35]).
[4] A. Gajewski, M. Zyczkowski, *Optimal Structural Design Under Stability Constraints*, Kluwer Academic Publishers, Dordrecht, The Netherlands, 1988.
[5] K. Federhofer, Uber die Querknickung gleichmässig gedrückter Kreisringe, *der Eisenbau* 12 (1921) 289–296.
[6] H. Hencky, Kippsicherheit und Achterbildung an geschlossenen Kreisringen, *Zeitschrift für angewandte Mathematik und Mechanik* 1 (1921) 451–455.
[7] S. Timoshenko, Kippsicherheit des gekrümmten Stabes mit kreisförmiger Mittelinie, *Zeitschrift für angewandte Mathematik und Mechanik* 3 (1923) 358–362.
[8] M. Farshad, On lateral–torsional instability of arches subjected to motion-dependent loading, *Journal of Sound and Vibration* 53 (2) (1977) 165–171.
[9] Z. Celep, On the lateral stability of a bar with a circular axis subjected to a non-conservative load, *Journal of Sound and Vibration* 66 (2) (1979) 219–225.

[10] N. Challamel, Discussion of: "a further study of flexural-torsional buckling of elastic arches," *International Journal of Structural Stability and Dynamics* 6 (1) (2006) 157–162.
[11] H. Ziegler, *Principles of Structural Stability*, Blaisdell Publishing Company, 1968.
[12] J.H. Michell, The small deformation of curves and surfaces with application to the vibrations of helix and a circular ring, *Messenger of Mathematics* 19 (1890) 68–76.
[13] E. Volterra, J.D. Morell, Lowest natural frequency of elastic arc for vibrations outside the plane of initial curvature, *Journal of Applied Mechanics* 28 (1961) 624–627.
[14] U. Ojalvo, Coupled twisting-bending vibrations of incomplete elastic rings, *International Journal of Mechanical Sciences* 4 (1962) 53–72.
[15] F.C. Nelson, Out-of-plane vibration of a clamped circular ring segment, *Journal of Acoustical Society of America* 35 (6) (1963) 933–934.
[16] P. Childamparam, A.W. Leissa, Vibrations of planar curved beams, rings and arches, *Applied Mechanics Reviews* 46 (1993) 467–483.
[17] T. Irie, G.Y. Yamada, K. Tanaka, Natural frequencies of out-of-plane vibration of arcs, *Journal of Applied Mechanics* 49 (4) (1982) 910–913.
[18] W.P. Howson, A.K. Jemah, Exact out-of-plane natural frequencies of curved Timoshenko beams, *Journal of Engineering Mechanics* 125 (1) (1999) 19–25.
[19] M.B. Rubin, E. Tufekci, Three-dimensional free vibrations of a circular arch using the theory of a Cosserat point, *Journal of Sound and Vibration* 286 (2005) 799–816.
[20] C.S. Huang, Y.P. Tseng, S.H. Chang, C.L. Hung, Out-of-plane dynamic analysis of beams with arbitrarily varying curvature and cross-section by dynamics stiffness matrix method, *International Journal of Solids and Structures* 37 (2000) 495–513.
[21] S.Y. Lee, J.C. Chao, Out-of-plane vibrations of curved non-uniform beams of constant radius, *Journal of Sound and Vibration* 238 (3) (2000) 443–458.
[22] V.V. Bolotin, *Nonconservative Problems of the Theory of Elastic Stability*, Pergamon Press, New York, 1963.
[23] A. Migliacci, Instabilità delle travi alte sotto carichi trasversali di tipo "non conservativo," *Il Cemento* 12 (1965) 17–27.
[24] M. Como, Lateral buckling of a cantilever subjected to a transverse follower force, *International Journal of Solids and Structures* 2 (1966) 515–523.
[25] G. Ballio, Sulla trave alta sollecitata da carichi di tipo non conservative, *Istituto Lombardo*, *Accademia di Scienze e Lettere, Estratto dai Rendiconti, Classe di Scienze (A)* 101 (1967) 307–330.
[26] G. Ballio, Sistemi aggiunti in problemi di stabilita' elastica in campo non conservato, *Istituto Lombardo*, *Accademia di Scienze e Lettere, Estratto dai Rendiconti, Classe di Scienze (A)* 101 (1967) 331–360.
[27] K. Wohlhart, Dynamische Kippstabilität eines Platenstreifens unter Folgelast, *Zeitschrift für Flugwissenschaften* 19 (1971) 291–298.
[28] Z. Celep, On the lateral stability of a cantilever beam subjected to a non-conservative load, *Journal of Sound and Vibration* 64 (2) (1979) 173–178.
[29] Z. Celep, On Prandtl's cantilever beam subjected to a bending moment, *Journal of Sound and Vibration* 71 (2) (1980) 185–190.
[30] F.M. Detinko, On the elastic stability of uniform beams and circular arches under nonconservative loading, *International Journal of Solids and Structures* 37 (2000) 5505–5515.
[31] D.H. Hodges, Lateral–torsional flutter of a deep cantilever loaded by a lateral follower force at the tip, *Journal of Sound and Vibration* 247 (1) (2001) 175–183.
[32] F.M. Detinko, Some phenomena for lateral flutter of beams under follower load, *International Journal of Solids and Structures* 39 (2002) 341–350.
[33] V.I. Feodosiev, *Advanced Stress and Stability Analysis*, Springer, Berlin, 2005.
[34] G.J. Simitses, D.H. Hodges, *Fundamentals of Structural Stability*, Elsevier, Burlington, 2006.
[35] Y. Wasserman, Spatial symmetrical vibrations and stability of circular arches with flexibly supported ends, *Journal of Sound and Vibration* 59 (2) (1978) 181–194.
[36] W.G. Godden, The lateral buckling of tied arches, *Proceedings of the Institution of Civil Engineers, Part III* (2) (1954) 496–514.
[37] R.H. Plaut, A. Hou, Deflections, vibrations, and stability of a pair of leaning arches, *Journal of Engineering Mechanics* 124 (7) (1998) 748–753.
[38] M.A. Bradford, Y.L. Pi, Elastic flexural-torsional instability of structural arches under hydrostatic pressure, *International Journal of Mechanical Sciences* 50 (2008) 143–151.
[39] F. Stüssi, Lateral buckling and vibration of arches, Publications, Vol. 7, Zürich, International Association for Bridge and Structural Engineering, 1944, pp. 327–343.
[40] F.J. Tokarz, Experimental study of lateral buckling of arches, *Journal of Structural Division* 97 (ST2) (1971) 545–559.
[41] C.F. Kee, The design of the unbraced stabbogen arch, *The Structural Engineer* (1959) 265–270.
[42] D.B. La Poutré, *Experimental testing of steel arches—Preliminary investigation*, Internal Report, Technische Universiteit Eindhoven, 2003, 42p.
[43] M.A. Langthjem, Y. Sugiyama, Dynamic stability of columns subjected to follower loads: a survey, *Journal of Sound and Vibration* 238 (2000) 809–851.
[44] I. Elishakoff, Controversy associated with the so-called "follower forces": critical overview, *Applied Mechanics Reviews* 58 (1–6) (2005) 117–142.
[45] A. Singh, R. Mukherjee, K. Turner, S. Shaw, MEMS implementation of axial and follower end forces, *Journal of Sound and Vibration* 286 (2005) 637–644.

[46] Y. Wasserman, The influence of the behaviour of the load on the frequencies and critical loads of arches with flexibly supported ends, *Journal of Sound and Vibration* 54 (4) (1977) 515–526.
[47] H. Wagner, *Torsion and Buckling of Open Sections*. NACA Technical Memorandum 807, 1936 (English translation by S. Reiss of Verdrehung und Knickung von offenen Profilen, from the 25th Anniversary Number of the Technische Hochschule, Danzig, 1904–1929, pp. 329–343).
[48] S.P. Timoshenko, J.M. Gere, *Theory of Elastic Stability*, McGraw Hill, New York, 1961.
[49] N.S. Trahair, *Flexural-torsional Buckling of Structures*, E&FN Spon, London, 1993.
[50] A.E. Love, *A Treatise on the Mathematical Theory of Elasticity*, fourth ed., Dover Publications, 1927.
[51] H. Leipholz, *Stability Theory*, Academic Press, London, 1970.
[52] G.M.L. Gladwell, Follower forces: Leipholz's early researches in elastic stability, *Canadian Journal of Civil Engineering* 17 (1990) 277–286.
[53] G.M.L. Gladwell, Follower forces: Leipholz's researches into generalized variational principles, *Canadian Journal of Civil Engineering* 17 (1990) 287–293.
[54] A.N. Kounadis, On the failure of static stability analyses of non-conservative systems in regions of divergence instability, *International Journal of Solids and Structures* 31 (15) (1994) 2099–2120.
[55] V.V. Bolotin, A.A. Grishko, A.N. Kounadis, C. Gantes, G.B. Roberts, Influence of initial conditions on the postcritical behaviour of nonlinear aeroelastic systems, *Nonlinear Dynamics* 15 (1998) 63–81.